Comparative study on 2D microseismic source location with synthetic seismograms recorded by borehole- and surface-receiver arrays

Anton Biryukov, Simon G.E. Harvey, Giovanni Grasselli
Department of Civil Engineering, University of Toronto

Summary

In this report an algorithm based on the finite difference approximation of the 2D acoustic wave equation has been implemented to create synthetic seismograms and perform the Reverse Time Migration (RTM) routine. A specific geometry, source input and on-surface noise conditions were introduced in the model. Based on the reversibility of wave equation, recorded waveforms were applied as a time-dependent boundary condition and extrapolated back in time to get the initial acoustic event location. The influence of a span between the receivers, influence of the velocity model and relative source-sensor position was investigated. The span less than 1.2λ was found fine enough for further wavefield analysis. The variations in borehole array depths showed the increasing quality of the reconstructed wavefield with the increase of the angular aperture. By running a hydraulic fracturing scenario based model, it was concluded that the criterion of focusing is the ultimate factor that must be thoroughly devised and implemented.

The resolution of the image depends on the dominant wavelength of the source. Thus the resolution may vary with changes in the dominant frequency of the source or velocity model. As spatial inaccuracy of the full waveform inversion depends on many factors, quantifying the uncertainty of the RTM is a complicated process and was out of the scope of this project.

Introduction

Brittle failures during hydraulic fracturing are often followed by microseismic events. Energy of those failures is released in the form of compressional and shear waves. Passive microseismic monitoring is based on recording the emitted waves and then utilizing their arrival times or full waveforms to estimate the location of the events. From the acoustic events distribution the dimensions and the fracture orientation can be deduced. One of important problems currently under discussion is the choice of acquisition geometry: what conditions favor surface versus borehole sensors deployment and data acquisition?

In the downhole case, the receiver array size and geometry is constrained by physical and operational limitations. Consequently, the array has a finite aperture with a small number of geophones. Decrease in the amplitude of events is caused mostly by geometric spreading or attenuation. If the sensors are deployed at the depth of the reservoir region subjected to fracturing, wave propagation is predominantly layer-parallel, resulting in less wave scattering [1]. It provides the lowest decay in the amplitude of events and the best view of a fracture's vertical dimension growth. Deep boreholes have the advantage of better signal-to-noise (SNR) characteristics and lower level of anthropogenic background noise, that allows accurate P- and S-waves arrival times to be picked.

In case of surface deployed receiver arrays, the noisy conditions in which the acoustic emission is recorded, play a big role in the emission source location. Using P-wave arrival times only also significantly reduces the sensivity to velocity model assumptions. Surface deployment has a more extensive azimuthal coverage and thus should improve hypocentre inversion [2].

Theory and Methods

For this case study, the dependence of the acoustic emission source location on the deployment geometry of sensors is investigated. The computational domain is represented by a rectangular 2000 m $\times$ 2000 m homogenous isotropic medium with a given velocity model, that resembles a vertical slice through the stimulated reservoir, where the upper boundary is a free surface (the surface of the earth). It was meshed into 160000 elements using an ordinary rectangular grid scheme with the element size $dh = 5$ m. To avoid undesirable non-physical reflections from the sides and the bottom which are assumed to be unbounded, absorbing boundary conditions should be implemented. Specifically, the boundary conditions derived by [3] were used.

To get the seismograms as the input for the further source location problem, the forward problem of wave propagation is first solved. The following wave equation is considered:

$$c_p(P_{zz} + P_{xx}) = P_{tt} \tag{1}$$

where P is pressure in compressional waves, the subscript indicates the partial derivative. After performing a central second order finite difference (FD) approximation, an explicit scheme for solving the wave propagation in time is derived:

$$\begin{gathered} P(x_k, z_j, t_{i+1}) = 2(1 - 2A^2)P(x_k, z_j, t_i) - P(x_k, z_j, t_{i-1}) \\ +A^2(P(x_{k+1}, z_j, t_i) + P(x_{k-1}, z_j, t_i) + P(x_k, z_{j+1}, t_i) + P(x_k, z_{j-1}, t_i)) \end{gathered} \tag{2}$$

where $A = c_p \frac{dt}{dh}$ is the Courant number, i, j, k are indexes of spatial and temporal grid points. To keep numerical simulation stable, the spatial grid size dh and temporal dt have to be adjusted so the Courant number for the model satisfies the criterion $A^2 < 0.5$ [4]. For numerical simulations described below with $dh = 5$ m, $dt = 1.4 * 10^{-3}$ s and $c_p = 2500$ m/s, A^2 was equal to 0.49, which guaranteed numerical stability throughout the calculation procedure. The input for a source used in this study was selected as a Ricker wavelet applied at a specific point(s). The source function and its spectrum are fully characterized by a single parameter–peak frequency and are illustrated in Figure 1.

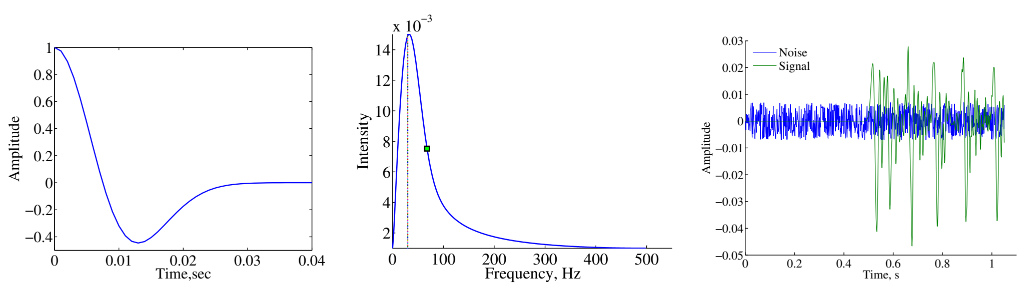

Figure 1. Ricker wavelet source function, its spectrum ($f_p = 30$Hz) and the signal with separated noise

The choice of a peak frequency is constrained by grid dispersion. Waves with high frequencies, having the shortest wavelengths will seem to slow down or even stop propagating once they get sampled less than six spatial samples per wavelength. Alford et al. [5] suggests $\frac{\lambda'}{dh} > 10$ for a second-order FD scheme, where λ' is the wavelength at the frequency of the upper half-power point (see Figure 1, green square). Otherwise in the presence of closely spaced events, grid dispersion may significantly distort the results leading to serious errors in interpretation of events.

To account for the noisy surface conditions, synthetical noise was superimposed on the seismic signal response (see Figure 1). Seismic noise is produced by a diversity of different unrelated and continuous sources and hence was modeled as a uniformly distributed random value to introduce sporadic "white" perturbation into the model. The final signal-to-noise ratio was set to 3.6.

The imaging of source parameters is based on the reversibility of the wave equation [6]. One of the principles of RTM was proposed by McMechan [7] and called Boundary Value Migration (BVM). The inversion problem is solved in the form of a boundary value problem. The acoustic emission sensors are placed along the boundaries of the domain. The seismograms recorded at every time step during the forward wave propagation modeling are reversed in time and then imposed as a time-dependent boundary condition, so that source configuration can be recovered by extrapolating the observation wave field back in time.

Examples

Influence of surface array density on RTM

The number of receivers on surface is usually redundant to mitigate the effect of high level noise on the results. Hence, it is worthwhile to observe how the quality of RTM changes with respect to the span between the receivers. The configuration of five sources in a line was chosen to demonstrate the dependence between source location accuracy and the span (Figure 2). Seismic events are clearly distinguished with spacing of 50 m and 100 m ($\sim 0.6\lambda_{dominant}$ and $\sim 1.2\lambda_{dominant}$, respectively) , whereas the abundant existence of artifacts with the span of 200 m and 250 m hinders the actual inversed source location.

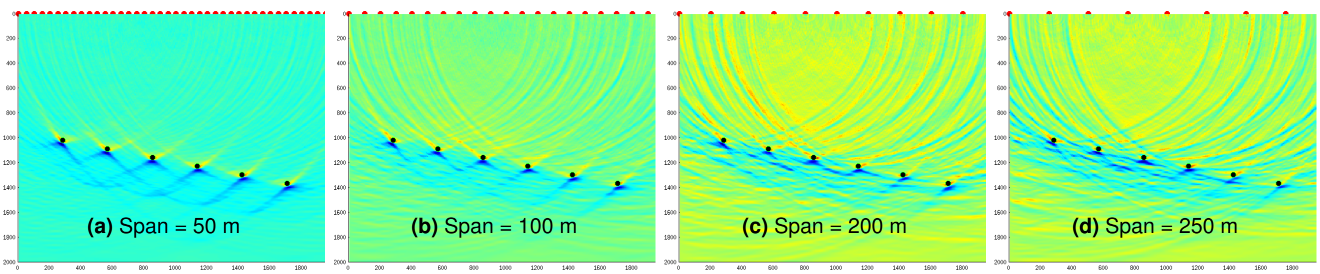

Figure 2. Influence of the spacing between receivers on the accuracy of location; black dots represent the origin of events, red dots - receivers involved.

Influence of borehole array depth on the RTM of successive acoustic events location

For this type of studies, four models with different depths of borehole array of receivers were simulated to observe how the quality of location depends on the respective distance between the sources and the array. There are also included results from two additional inversion attempts: a) utilizing two borehole arrays at the same time and b) utilizing surface array. As an attempt to reproduce realistic seismic response during hydraulic fracturing the sequence of 7 microseismic events following hypothetical hydraulic fracture propagation trajectory was introduced with a short time delay of $\frac{1}{21f_{peak}}$ between two successive events.

The angular aperture of the source can be defined as an angle formed by the uppermost sensor, the source, and the lowermost sensor. In Figure 4 one can notice that as the borehole sensors are moved downwards from the surface and the angular aperture between the source and the array increases, the smearing reaches its minimum at the maximum angular aperture, when the source is in the depth interval of the sensors. It correlates well with the source (namely, third from the left side) angular aperture change plotted in Figure 3, showing that the least smearing can be achieved with the first sensor deployed at 830 m, where the approximately maximum angular aperture is reached.

The seismograms recorded by the array with the first sensor at 1250 m are illustrated in Figure 3. The resultant source locations after inversion procedure using borehole arrays are shown in Figure 4.

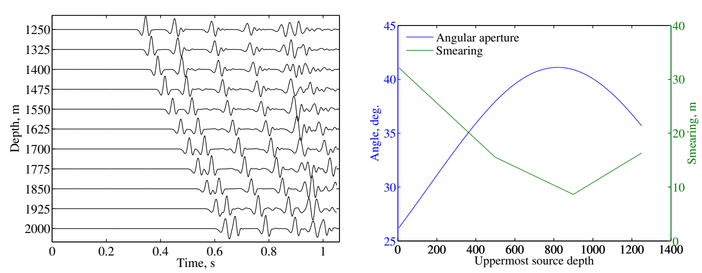

Figure 3. Synthetic seismograms recorded by borehole array and spatial smearing and the angular aperture as a function of the borehole array depth

The recorded data was extrapolated back in time up to the moment when the first acoustic event occurred. It is noteworthy that the BVM technique utilized for the inversion procedures mentioned shows sensitivity towards time delay between the events. Moreover, it is observed (Figure 4) that as the time difference between the first and any other chosen event increases, the error of its location becomes larger and the question of the moment to stop waveform back-in-time extrapolation raises. Thus, to more accurately estimate the location of the acoustic event using RTM methods, the preliminary seismogram analysis and time of occurrence picking procedure should be properly conducted. This will give a chance to properly constrain the moment of maximum focus for a particular event occurred at the moment of time picked from the records. One of the possible ways to organize that could be solving a triangulation problem first to have a first guess for the moment of source occurrence and then compare location results yielded by triangulation method with RTM up to the same moment.

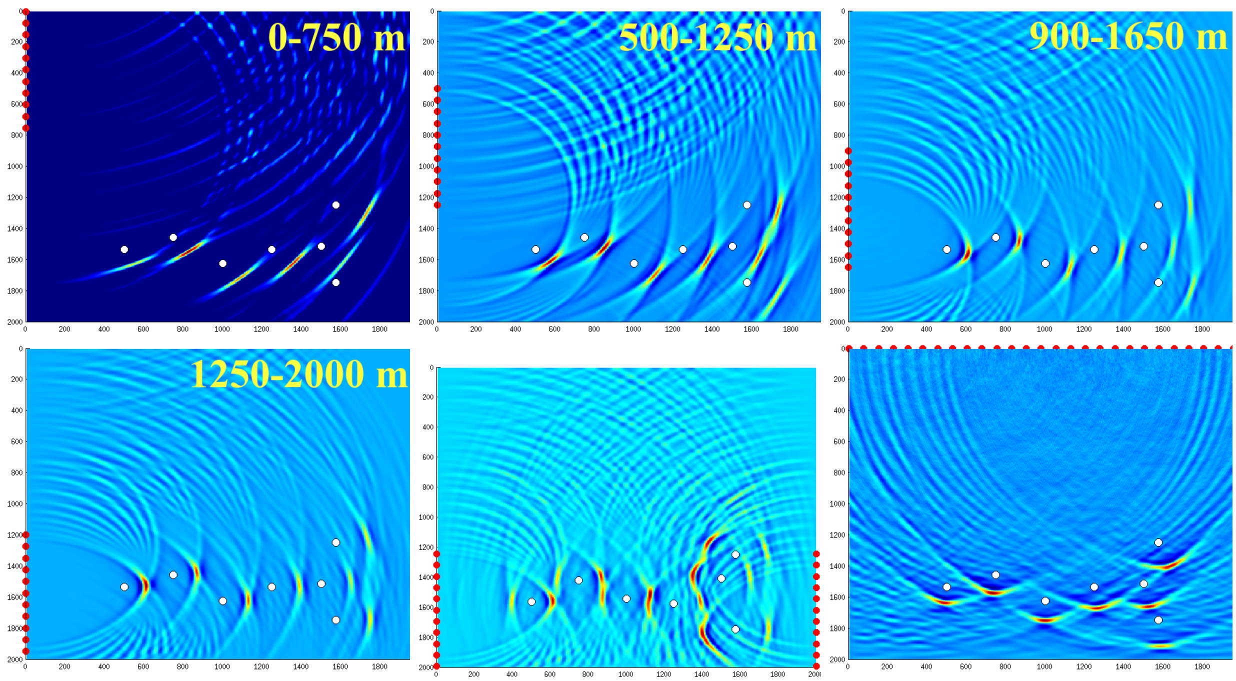

Figure 4. The influence of borehole vertical array depth on the location accuracy of temporarily close events using **borehole sensors**; receivers are shown with red dots, actual sources' locations - with white dots

Influence of Velocity Model on the RTM of acoustic events location

Building accurate, high-resolution velocity models involves an iterative process of structural interpretation and modeling, velocity and anisotropic parameter analysis and modeling, and velocity updates. A complete discussion of velocity model building is out of the scope of this paper, but it is worthwhile to show the effects of an erroneous velocity model to emphasize its importance. A 2D velocity model of an anticlinal petroleum reservoir comprised of a limestone reservoir overlain by a 200 m thick anhydrite caprock, overlain by a succession of limestone rocks is used for demonstration. The rock type p-wave velocities are given below in Figure 5, and are taken after the range of typical rock type velocities provided in [8]. A velocity gradient ranging from 3500 m/s at surface to approximately 4700 m/s at depth has been applied to the succession of limestone units, simulating the common increase in p-wave velocity with depth due to the effects of increased lithification and compaction [9]. The same 5 source locations were used, and the RTM was done with velocity errors of 5% and 10% (Figure 6). It is notable that for velocity models with overestimated velocity, the seismic event location is too shallow, and vice versa for velocity underestimates. This is the result of increased refraction with increasing velocity for the ray path through the curved strata, which act as a focusing lens for the RTM waveforms. However, the seismic source x-coordinate is quite robust, regardless of the velocity model.

Conclusions

For this project, a two-dimensional, second-order, time-explicit finite difference approximation of the acoustic wave equation was developed to model the propagation of microseismicity-associated acoustic waves

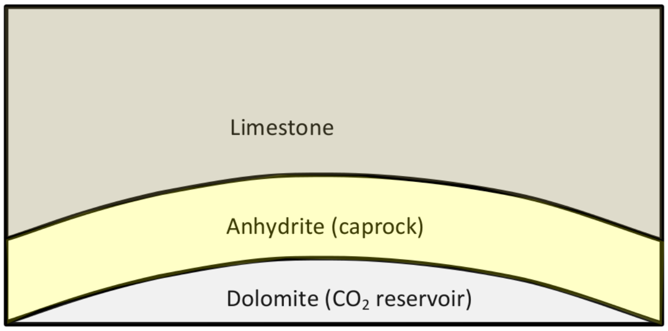

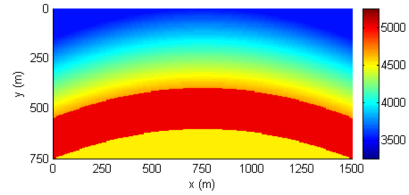

Rock Type	v_p (m/s)	Model v_p (m/s)
Limestone	3500-6000	3500-4700
Anhydrite	4000-5500	5000
Dolomite	3500-6500	4500

Figure 5. Diagrammatic representation of the anticlinal hydrocarbon reservoir with the associated velocity model and rock type p-wave velocity table.

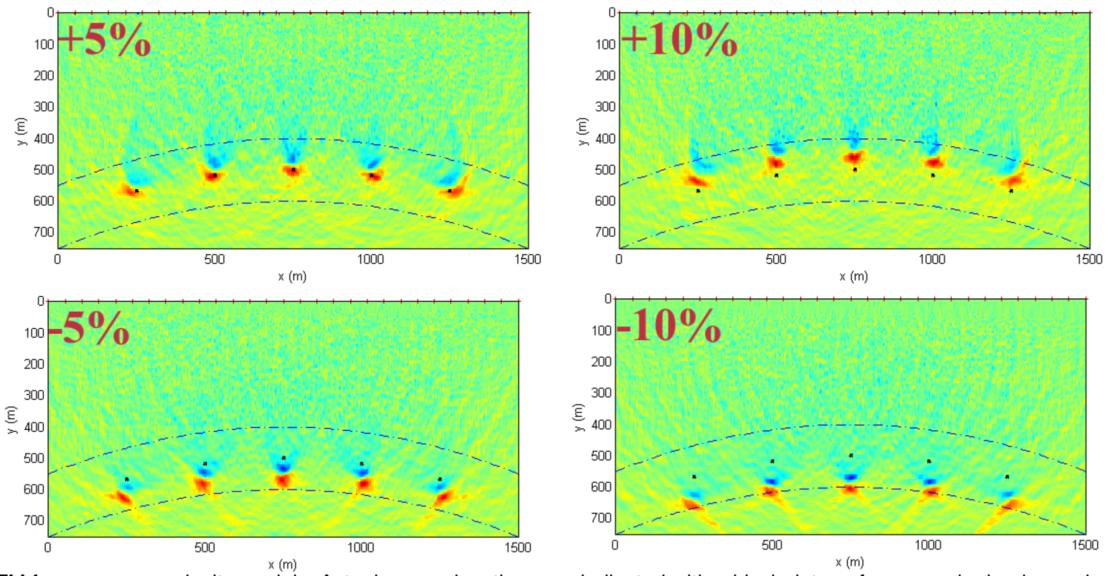

Figure 6. RTM for erroneous velocity models. Actual source locations are indicated with a black dot, surface array hydrophones by a vertical red line and the anhydrite layer by a dashed blue line.

through geologic media. Subsequently, by recording pressure values along the chosen boundaries during forward migration and applying them in reverse as a time-dependent boundary condition, reverse time migration (RTM) of the waveforms to the original source was accomplished. Anthropogenic noise was introduced to the seismic signals by means of uniformly distributed random numbers, an appropriate analog to the stochastic nature of seismic noise. The scope of the project was to explore the influence of a span between the receivers, influence of the velocity model and relative source-sensor position on the RTM source location. For the given model characteristics, it was found that the effect of noise was negated for array sensor spacing of 1.2λ and under. The effect of an inaccurate velocity model was investigated; due to the focusing lense effect of the curved strata, velocity overestimates led to source depth underestimates, and vice versa for velocity underestimates. The horizontal location was found to be quite robust, regardless of velocity model errors. An analysis of the RTMs spatial resolution revealed that the source dominant wavelength defines the minimum spacing of visually distinguishable simultaneous seismic events.

The variations in borehole array depths showed the increasing quality of the reconstructed wavefield with the increase of the angular aperture. By running a hydraulic fracturing scenario based model, it was concluded that the criterion of focusing is the ultimate factor that must be thoroughly devised and implemented.

Acknowledgments

The authors would like to express gratitude to Ramin Saleh and Qi Zhao of the University of Toronto's Physics and Civil Engineering Departments, respectively, who were of tremendous help throughout the project.

References

[1] Mirko van der Baan, David Eaton, and Maurice Dusseault. Microseismic monitoring developments in hydraulic fracture stimulation. *Effective and Sustainable Hydraulic Fracturing*, pages 439–466, 2013.

[2] D.W. Eaton and F. Forouhideh. Microseismic moment tensors: The good, the bad and the ugly. *CSEG Recorder*, 9(35):45–49, 2010.

[3] Robert Clayton and Björn Engquist. Absorbing boundary conditions for acoustic and elastic wave equations. *Bulletin of the Seismological Society of America*, 67(6).

[4] A. R. Mitchell. *Computational Methods in Partial differential Equations*. John Wiley & Sons.

[5] R. M. Alford, K. R. Kelly, and D.Mt Boore. Accuracy of finite-difference modeling of the acoustic wave equation. *Geophysics*, 39(6):834–842, 1974.

[6] Jean-Pierre Fouque. *Wave propagation and time reversal in randomly layered media*. Springer, New York, 2007.

[7] G.A. MCMECHAN. Migration by extrapolation of time-dependent boundary values. *Geophysical Prospecting*, (31):413–420, 1983.

[8] J. C Jaeger, Neville G. W Cook, and Robert Wayne Zimmerman. *Fundamentals of rock mechanics*. Blackwell Pub., Malden, MA, 2007.

[9] L. Y. Faust. A VELOCITY FUNCTION INCLUDING LITHOLOGIC VARIATION. *GEOPHYSICS*, 18(2):271–288, April 1953.